

PAPER • OPEN ACCESS

Test of a DC-HTS Busbar Demonstrator for Power Distribution in Hybrid-Electric Propulsion Systems for Aircraft

To cite this article: S I Schlachter *et al* 2022 *IOP Conf. Ser.: Mater. Sci. Eng.* **1241** 012037

View the [article online](#) for updates and enhancements.

You may also like

- [The Cell Cooling Coefficient: A Standard to Define Heat Rejection from Lithium-Ion Batteries](#)
Alastair Hales, Laura Bravo Diaz, Mohamed Waseem Marzook *et al.*
- [Light Assisted Electrodeposition and Silicidation of Ni for Silicon Photovoltaic Cell Metallization](#)
Qiang Huang, Satyavolu S. Papa Rao and Kathryn Fisher
- [Pathway towards 24% efficiency for fully screen-printed passivated emitter and rear contact solar cells](#)
Yuchao Zhang, Li Wang, Daniel Chen *et al.*



The Electrochemical Society
Advancing solid state & electrochemical science & technology

243rd ECS Meeting with SOFC-XVIII

More than 50 symposia are available!

Present your research and accelerate science

Boston, MA • May 28 – June 2, 2023

[Learn more and submit!](#)

Test of a DC-HTS Busbar Demonstrator for Power Distribution in Hybrid-Electric Propulsion Systems for Aircraft

S I Schlachter¹, J Brand², S Elschner³, S Fink¹, B Holzapfel¹, A Kudymow¹, J Willms¹

¹ Karlsruhe Institute of Technology, Institute for Technical Physics, Hermann-von-Helmholtz-Platz 1, 76344 Eggenstein-Leopoldshafen, Germany

² Ingenieurbuero Brand, Karlstrasse 8, 68794 Oberhausen, Germany

³ University of Applied Science, Paul-Wittsack-Str. 10, 68163 Mannheim, Germany

Corresponding author: sonja.schlachter@kit.edu

Abstract. In the framework of the German project TELOS (Thermo-Electrically Optimised Aircraft Propulsion Systems) a high-temperature superconducting 40 MVA DC demonstrator busbar for hybrid-electric propulsion systems for aircraft has been developed. The design current for a temperature below 25 K is 13.3 kA and the rated voltage is 3 kV. The 2-pole busbar contains 2 stacks of REBCO coated conductors which are supported by a 3D-printed structure allowing compensation of thermal length changes of the superconductor. It fits in a cryostat tube with an inner diameter of 25 mm. A special focus has been put on low-resistive joints that are necessary to connect single elements of the busbar system. The special layout of the joints allows an effective current redistribution between the different tapes in a stack. We present results for the test of the DC busbar demonstrator in liquid nitrogen at 77 K. The design current for this temperature is 3.3 kA which corresponds to a rated power of 10 MW. We applied currents up to 3.5 kA and measured the I-V characteristics and contact resistances of 90° and 180° joints in a virgin and in a strained state thus simulating thermal length changes. We also present results of Lorentz-Force tests with short AC current pulses up to 20 kA to demonstrate the viability of the design for application with currents up to 13.3 kA.

1. Introduction

The climate change caused by the increasing emission of greenhouse gases is affecting people all over the world. In 2015 the civil and military air traffic contributed 875 million tons of CO₂, i.e. about 2.5%, to the global anthropogenic CO₂ emissions [1]. The predicted yearly growth in air-travel is 4-5 %, i.e. the global flight demand doubles every 15 years [2]. In order to keep further temperature increases due to the greenhouse effect on an acceptable level, greenhouse gas emissions, e.g CO₂ or NO_x, have to be reduced drastically. In “Flightpath 2050” the European Commission has set goals for the aviation industry to be reached until 2050: 75% reduction in CO₂ emissions per passenger kilometer, 90% reduction in NO_x emissions, emission-free aircraft movements when taxiing and reduction of noise emission of flying aircraft by 65% - all numbers compared to a typical new aircraft of the year 2000 [3]. Reaching these ambitious goals just by increasing the efficiency of today’s technologies is very difficult – rather a breakthrough of new technologies for the aviation sector is needed. One promising way to achieve the goals of “Flightpath 2050” is the electrification of aircraft propulsion systems, however,



batteries are too heavy to power drive trains with power in the range of several 10 MW. Hybrid-electric propulsion systems with gas turbine and generator allow generation of power in the required range on board of the aircraft. Superconductivity would substantially support this technology, because components of the drive-train like motors, generators and cables could be realized with improved power-to-weight ratios. Using cryogenic hydrogen both as coolant and fuel would result in an effective reduction of greenhouse-gas emissions. In the framework of the German project “TELOS” (Thermo-Electrically Optimised Aircraft Propulsion Systems) six partners, Airbus Group Innovations, Airbus Operations GmbH, Karlsruhe Institute of Technology, Siemens AG, Neue Materialien Bayreuth GmbH, and Technical University of Munich, joined in 2016 to develop a technological basis for a hybrid electric propulsion system for aircraft on an appropriate power level for the high power class.

A basic architecture for a cryogenic hybrid-electric propulsion system is described in detail in [4]. Two power generation units with superconducting generators which are driven by turboshaft engines are placed in the fuselage of the aircraft. The electric propulsion units (EPUs) which deliver the required thrust with superconducting motors and fans are placed in the wings of the aircraft. A DC power-distribution system with cryogenic AC/DC and DC/AC converters connect the generators and EPUs.

In this paper we focus on results obtained within the work package “Conductor Technology” in which a superconducting power distribution system for the hybrid-electric propulsion system should be developed. Originally the rated power was set to a value of 10 MW in the TELOS-project, however, to cover the requirements for the electrification of the Airbus A320 class the targeted power was later increased to a value of about 40 MW in the framework of “TELOS-Upgrade”, an amendment to the original TELOS project.

The paper is arranged as follows: In section 2 the design of the two-pole DC cable is described briefly and results from a self-consistent calculation of critical currents, magnetic fields and Lorentz forces are presented. Low-resistive joints are required to connect different cable sections. Results for joints which allow current redistribution between different tapes of a single pole are described in section 3. In section 4 the test of a short demonstrator cable in liquid nitrogen is presented and test results are being discussed.

2. Power distribution system

In the framework of the TELOS project a DC power distribution system on the basis of high-temperature superconductors should be developed. The advantage of a DC architecture is the decoupling of power and thrust generation units by power electronic converters which allow running generators and motors at an appropriate speed as required by the varying phases during the flight [5]. E.g. it is possible to run the generator at high speed while the motors run at lower speed with higher torque. In case of distributed propulsion systems with many motors it is also possible to run the motors at different speed, e.g. during the cruise phase. Another advantage of DC power distribution are the reduced AC losses. Even in DC distribution systems AC losses cannot be avoided completely as the rectified signal usually contains residual ripples. However, as the ripple amplitude in the rectified signal is usually small compared to the original AC amplitude, even superconductor cable architectures like stack cables can be applied.

2.1. Cable Layout

We decided to design the DC power distribution system as a busbar system with two poles (+1.5 kV, -1.5 kV) in one cryostat. A simple stack architecture for the two poles of the cable was chosen (Figure 1 and Figure 2). This allows to change the number of tapes easily to account for changed specifications with respect to current carrying capability of the cable and also for differences in the quality of commercial superconductors. In order to minimize size and weight of the cable we decided to limit the outer dimensions of the cable assembly including superconducting tapes and 3D printed wave-guide structure to a maximum diameter of 25 mm because in TELOS we used standard steel tubes with inner diameter of 25 mm as inner cryostat tube as shown in Figure 2.

To account for simple transportation and installation, the busbar system consists of single elements with a maximum length of 6 meters. In order to connect single elements, low-resistive 180°-, 90°- and

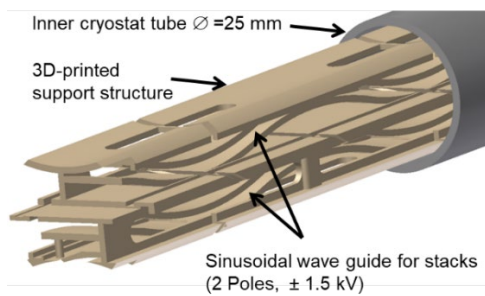


Figure 1: CAD drawing of inner cryostat tube and 3D-printed former with wave-guide for REBCO tape stacks .

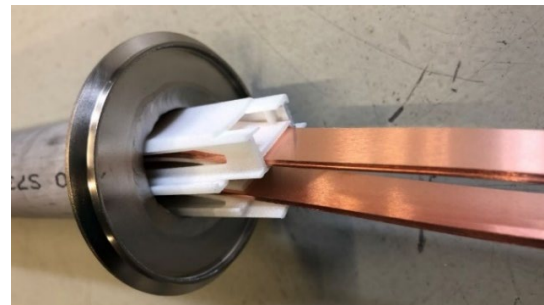


Figure 2: Photograph of inner cryostat tube with 3D-printed former and a tape stack for each pole of the cable.

T-joints had to be developed. The stack design of our two-pole cable allows face-to-face connection of the superconducting tapes so that low resistive joints could be realized.

We also decided to compensate thermal length changes of the cold cable sections within the busbar structure, avoiding compensation elements at the cable ends with a size that depends on the cable length. Compensation of thermal length changes was achieved by placing the stacks in a 3D-printed support structure made of glass-bead filled polyamide 12 with sinusoidal wave guides for the stacks. Contraction of the HTS-tapes during cool-down can easily be compensated by a change of the wave amplitude. The former not only helps to compensate thermal length changes, but also ensures that the distance between the stacks is kept constant and that the REBCO stacks do not touch the inner cryostat tube.

We made several high-voltage tests to ensure that the cable-design is suitable to withstand voltages of 3 kV and more between the two poles or between one pole and the inner cryostat tube. The tests were made at room temperature in air atmosphere as a worst-case scenario. No voltage breakdowns happened at 3 kV with exception of one sample joint damaged by welding which needed repair. Voltage breakdowns appeared in air on few samples for values between 4 kV and 5 kV. However, under the foreseen operation conditions with subcooled nitrogen or liquid hydrogen the high voltage breakdowns can be expected to appear at much higher values. Fault scenarios with fluid and pressure loss would require an adapted improvement of the high voltage design.

2.2. Critical currents, magnetic fields and Lorentz forces

To calculate the current carrying capacity, the field distribution and the Lorentz forces due to the self-field for the 2-pole HTS cable, an existing MATLAB code was modified [6]. The self-consistent model uses the E - J relationship $E/E_c = (J(B)/J_c(B))^n$ for superconductors where E is the electric field, E_c the electric field criterion to determine the critical current density J_c , B is the magnetic flux density and the exponent n is a measure for the homogeneity of the material and the steepness of the transition from superconducting to normal behavior. As the current carrying capacity of REBCO superconductors is strongly dependent on temperature, magnitude and direction of the magnetic field, we used a parameter-free routine described in [7] to calculate the $J_c(B, \theta)$ dependence for a Theva ProLine conductor¹ for which experimental $I_c(B, \theta)$ data were available from the HTS database of the University of Wellington [8]. We mainly concentrated on two different application cases which represent the goals of the two project phases, TELOS and TELOS-Upgrade: distribution of a nominal power of 10 MW with an LN₂ cooled cable system (subcooled pressurized LN₂, $T \approx 70$ K) and distribution of a nominal power of 40 MW with a hydrogen cooled cable system at ($T \approx 20$ -25 K). For both application cases a voltage of 3 kV (± 1.5 kV) was assumed, resulting in nominal currents of 3.33 kA and 13.33 kA for electric power levels of 10 MW and 40 MW, respectively.

¹ THEVA Pro-Line 2G HTS Wire, TPL4420c, Manufacturer sample designation: ID 180152

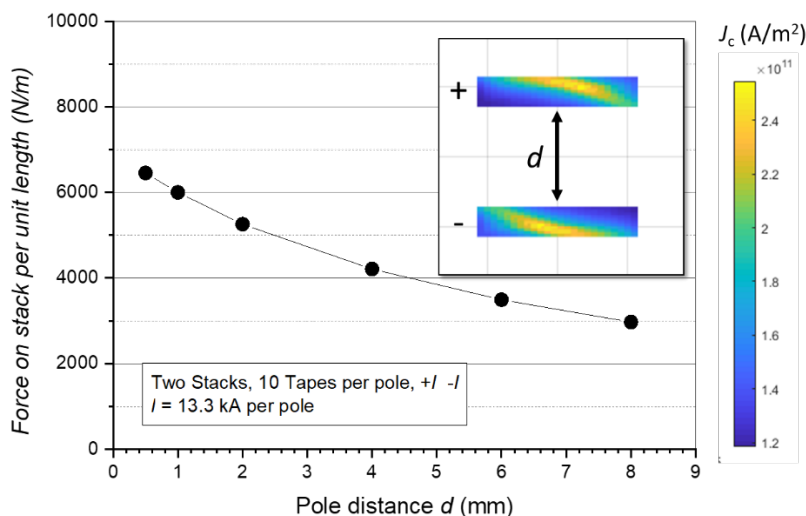


Figure 3: Calculated Lorentz forces on single stacks of a 2-pole stack cable versus stack distance for a current of 13.3 kA. The inset shows the absolute values of the calculated current density distribution in the stacks of the cable with Theva-ProLine-conductor at $T = 20$ K. The calculated current density corresponds to an assumed REBCO-layer thickness of $1 \mu\text{m}$. Real Theva conductors have REBCO layer thicknesses in the order of $3 \mu\text{m}$, i.e. the real current densities are approx. a factor 3 lower.

In a first step we assumed having a cable with two stacks of 12 mm wide REBCO tapes, one for each pole of the cable. Each tape stack consists of 10 REBCO tapes. We calculated current densities, magnetic field distributions and Lorentz forces for different distances of the two stacks and for different temperatures. The current distribution in the two poles of the cable calculated for a temperature of 20 K is shown in the inset of Figure 3 (absolute values). The distribution is not symmetric with respect to the x -axis which is parallel to the tape surface. This is a consequence of the c -axis tilt of the superconductor layer due to the inclined substrate deposition process applied by Theva [9]. Due to the different opposite current directions in the two stacks, the magnetic field strength is high between the two stacks and decreases very fast outside the stack assembly, resulting in low stray fields outside the cryostat. The asymmetric current distribution results in Lorentz forces which do not only act in the y -direction on the tapes (perpendicular to the tape plane), but also in the x -direction, i.e. parallel to the tape plane. Therefore, the two stacks need to be stabilized not only against the repelling forces perpendicular to the tape plane, but also against forces parallel to the tape plane. In Figure 3 the Lorentz force on a single stack is shown as a function of the stack distance. If the stacks are close together the forces per unit length exceed values of 6 kN/m for a current of 13.33 kA corresponding to a power level of 40 MW at

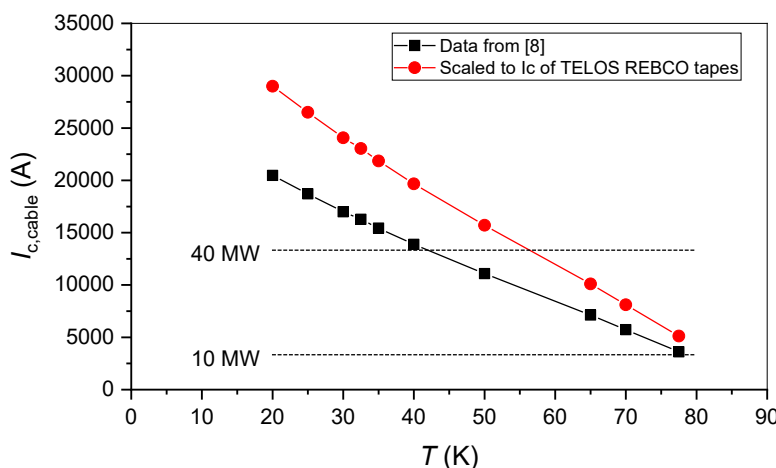


Figure 4: Calculated critical currents for a 2-pole cable with 10 Theva ProLine tapes in each stack (stack distance = 7 mm). The black squares were obtained from calculations with $I_c(B, \theta)$ data from [8] while the red circles were obtained by scaling these data to the higher current carrying capability of the Theva tapes used within the TELOS project.

3 kV. In order to minimize the Lorentz forces as much as possible we used a stack distance of 7 mm for our cable, resulting in Lorentz forces of 3.2 kN/m on the stacks. This allowed us to realize the wave-like guiding of the stacks for compensation of thermal length changes still keeping the diameter of the cable assembly of support structure and REBCO stacks below our limit of 25 mm.

Figure 4 shows the critical currents of the cable calculated with temperature dependent $I_c(B, \theta)$ data from [8] for different temperatures. According to the calculations, critical currents of 5.7 kA and 20.4 kA can be achieved at temperatures of 70 K and 20 K, respectively, with 2×10^{12} mm wide Theva ProLine tapes. For the two application cases, power distribution of 10 MW at 70 K and 40 MW at 20 K, the cable would operate at 58% and 65% of the critical current, respectively. The Theva conductors that have been used in the TELOS-project, have an approximately 40% higher current carrying capability than the conductor from Ref. [8]. Therefore, we simply scaled the calculated data to the current carrying capability of our tapes to see up to which temperatures our cable could operate with currents of 3.3 kA and 13.33 kA. An electrical power of 10 MW could be distributed up to temperatures of ~ 80 K and a power of 40 MW up to temperatures around 55 K.

3. Joints

Since a modular structure is intended for the cable in the aircraft, it is necessary to provide couplings between such modules. 180° -connections as well as 90° - and T-joints are necessary, and in the long term any angular connections could be required. Besides cryostat and ripple losses, resistive joints are a major source of losses in DC cables. Especially at low temperatures, the cooling penalty is high due to the low Carnot efficiency and small amounts of heat can lead to strong temperature increases. In aerospace applications cooling power is usually limited because either a cryogen has to be carried on board the aircraft or space vehicle or the electric energy for mechanical coolers needs to be provided. To keep losses at a minimum, we set an upper limit for the losses of joints in our busbar system. Resistive losses of a joint in one pole should be below 1 W, i.e. a 2-pole cable coupling should have resistive losses below 2 W. For a current of 13.33 kA the resistance of a single joint thus needs to be below 5.6 n Ω . As a comparison, the heat load per unit length of commercial cable cryostats, are often in the range of 1-2.5 W/m [10].

In the past, it has been demonstrated that REBCO tapes can also be superconductively connected. Park et al. achieved a resistance $< 10^{-17} \Omega$ for a joint of $\text{GdBa}_2\text{Cu}_3\text{O}_{7-\delta}$ tapes [11]. However, for connecting two cable ends during installation in an aircraft, this complex process of contacting is not suitable. To achieve low-resistive joints between two REBCO tapes, face-to-face (ftf) soldering, i.e. soldering the tapes with the superconductor sides together is commonly used. Resistances of $R \cdot A$ (A = contact area) in the range of several 10 n $\Omega \cdot \text{cm}^2$ have been obtained for joints between single tapes, however, the achievable values also depend on the interlayer resistances between REBCO layer, silver layer and Cu layer and depend strongly on the manufacturing process [12].

One major problem in stacks of REBCO tapes is the redistribution of currents, due to the insulating buffer layers in the REBCO tapes. While currents flowing from one tape to the other can cause resistive losses especially in AC applications, DC applications can benefit from the possibility of current redistribution in case of single tape failure (e.g. due to local heating, mechanical damage or varying magnetic fields along the cable length). As the tapes in the stacks of the TELOS cable are only loosely

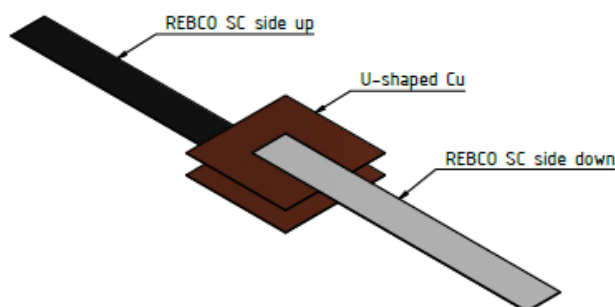


Figure 5: Face-to-Face soldering of i^{th} tape of stack S1 to i^{th} tape of stack S2 ($i=1-10$). U-shaped Cu plates were added to facilitate transverse current flow between tapes in different layers of the stack.

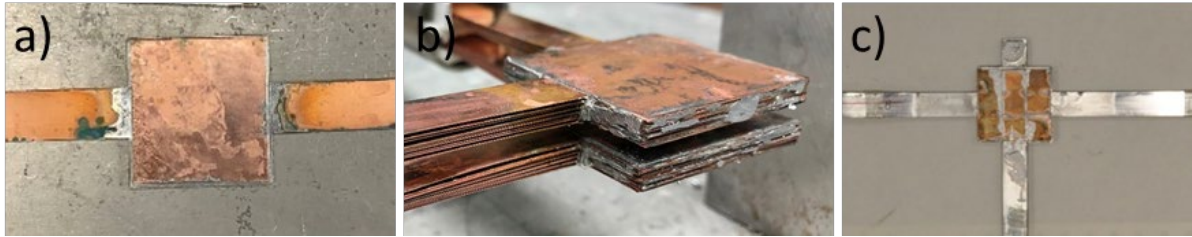


Figure 6: Joints of stacks with ten 12 mm wide tapes, REBCO tape overlap area of 12 x 12 mm² and a total joint area of 36 x 36 mm² : a) 180° joint, b) the two 90° joints of the 2 poles of the TELOS cable demonstrator, and c) T-joint of two stacks.

connected throughout the cable section, a good connection of the tapes in the joint sections can facilitate current redistribution. We developed a special technique to connect the i^{th} tape of a stack S1 with the i^{th} tape of a second stack S2 (i : number of layer in stack, $i=1 \dots 10$) by direct ftf soldering to achieve low longitudinal resistances while ensuring also low transverse resistances between the single tapes. We used an overlap length of the two stacks which equals the tape width, i.e. the contact area was 12 mm x 12 mm in the case of 180° joints as well as in the case of 90° joints. In order to facilitate the transverse current flow, we added U-shaped Cu plates (size 36 mm x 36 mm) in each layer of the stack (Figure 5).

Before the final assembly of the cable demonstrator we fabricated several 180°- and T-joints and measured the longitudinal and transverse resistances. We used 12 mm wide tapes from SuperPower (50 μm substrate thickness) or Theva (100 μm substrate thickness) with 20 μm surround Cu coating. The thickness of the U-shaped Cu plates was 100 μm and 170 μm for joints with SuperPower and Theva tapes, respectively. Sn63Pb37 foil was used as solder between the single REBCO/Cu layers in the joint. The longitudinal and transverse resistances between single tapes of two different stack joints with SuperPower tapes are shown in Table 1 and Table 2.

Table 1. Measured resistances R ($10^{-9} \Omega$) between single tapes from stack S1 layer L_n and stack S2 layer L_m for joint #1 .

R ($10^{-9} \Omega$)	S2-L1	S2-L2	S2-L5	S2-L6	S2-L10
S1-L1	46	78	218	236	327
S1-L2	105	42	168	190	286
S1-L5	206	152	39	89	232
S1-L6	243	195	108	38	198
S1-L10	345	300	250	216	39

Table 2. Measured resistances R ($10^{-9} \Omega$) between single tapes from stack S1 layer L_n and stack S2 layer L_m for joint #2 .

R ($10^{-9} \Omega$)	S2-L1	S2-L2	S2-L5	S2-L6	S2-L10
S1-L1	45	93	220	232	330
S1-L2	117	44	166	180	286
S1-L5	210	151	39	77	229
S1-L6	238	186	98	43	197
S1-L10	360	313	260	228	60

Both joints were soldered simultaneously in a specially constructed soldering device to simulate the soldering process in a 2-pole cable. The longitudinal and transverse resistances between five of the tapes of each stack were determined in LN₂ by applying currents between two single tapes of the stacks and measuring the voltage drops. The longitudinal resistance values of the direct ftf transitions within a stacking plane (i.e. between layer i of stack S1 and layer i of stack S2) are in the range of 38-60 n Ω . The

average values for joint #1 and joint #2 are 40.8 nΩ and 46.2 nΩ, respectively, corresponding to total longitudinal joint resistances of 4.08 nΩ and 4.62 nΩ for the parallel connection of the ten such fff connections in the joints of stacks with 10 tapes. The resistive losses for such a joint would be below 1 W for a current of 13.3 kA, i.e. below the maximum value set as a goal for the TELOS cable. Taking the decreasing resistivities of metallic components in the joints into account when going from 77 K to 20 K the losses should become even smaller for applications in liquid hydrogen. The transverse resistances between tapes of different layers increase with increasing layer distance, being in the range of 327-360 nΩ for the outer tapes of the stack, i.e. between tapes of layer 1 and layer 10. For T- and 90°-joints we observed similar resistance values as for 180° joints. The low transverse resistances allow the redistribution of currents within the joints.

4. TELOS SC Cable Demonstrator

In the framework of TELOS-Upgrade a superconducting demonstrator cable was designed for a power transmission of 40 MW at $T = 20\text{-}25\text{ K}$ (hydrogen cooling). This power corresponds to a current of 13.33 kA at a nominal voltage of 3 kV. Since it was not possible to realize hydrogen cooling within the time and budget framework of the TELOS project, it was already decided in the application phase of TELOS-Upgrade to test the demonstrator cable in a nitrogen bath at 77 K. A nominal current of $I_{\text{nom},77\text{K}} = 3333\text{ A}$ was targeted for this test, which would correspond to a transmission power of 10 MW at $U_{\text{nom}} = 3\text{ kV}$. This power corresponds to the value that was originally targeted before the realignment through the TELOS-Upgrade. With the proof of a current-carrying capacity of $I_{\text{nom},77\text{K}} = 3.33\text{ kA}$ at $T = 77\text{ K}$ and the assumption of an at least 5 times higher current-carrying capacity at $T = 20\text{ K}$ as shown in Figure 4, indirect proof of a sufficient current-carrying capacity at 20 K can thus be provided. Besides the demonstration of sufficient current carrying capability one of the major goals was to demonstrate the realization of low-ohmic joints with resistances below 5.6 nΩ. Therefore, the 2-pole demonstrator cable was designed with 3 superconducting cable sections connected by 180°- and 90°-couplings and a short-circuit connection at one end (Figure 7). A special device for straining SC section 2 was built to demonstrate compensation of thermal length changes by wave-like guiding of the REBCO stacks. A major goal for the test of the demonstrator cable was the proof that it can withstand the high Lorentz forces acting on superconductors and support structure at $I = 13.33\text{ kA}$. Lorentz force tests at 77 K were carried out with 50 Hz AC currents with amplitudes up to 20 kA and a limited duration of 40 ms. The maximum currents in these tests were far above the critical current of the cable, however, since the pulse duration was very short, the cable was not expected to be destroyed by the thermal load. The following series of tests was made: DC test #1 up to $I = 967\text{ A}$ (test measurement, then minor modifications to the measurement program), DC test #2 up to $I = 3450\text{ A}$, DC test #3 (current ramp to 1 kA, stretching of

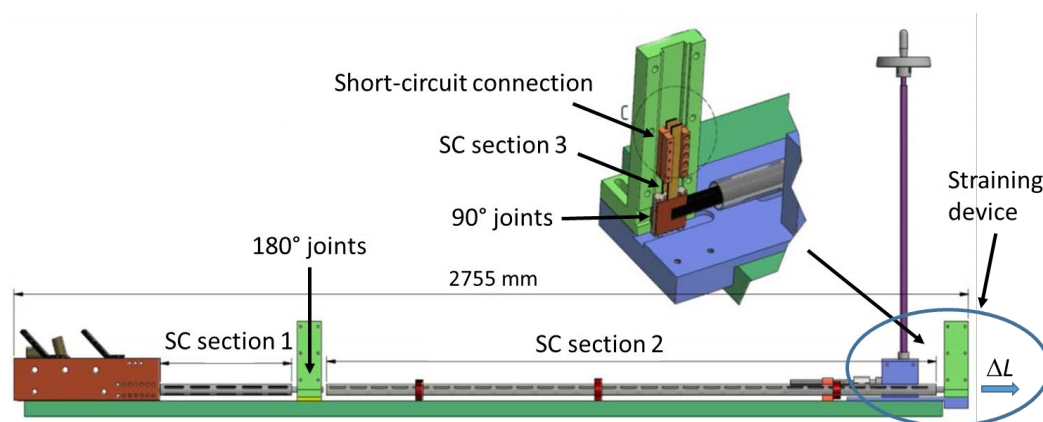


Figure 7: CAD drawing of the 2-pole TELOS demonstrator cable consisting of 3 SC cable sections connected with 180°- and 90°-joints. The two poles of the cable are connected with a short-circuit connection at one cable end. Length changes of SC section 2 (length = 1.8 m) can be performed with the straining device.

cable with $\Delta L=+7$ mm then current ramp up to 3410 A), Lorentz force test up to 20 kA (AC, 40 ms), DC test #4 up to $I = 3500$ A and DC test #5 up to $I=3470$ A.

4.1. Initial DC test

Figure 8 shows the voltage drops measured at the 2 poles of 3 superconductor (SC) sections during DC test #2. Although the sample voltages did not show any abnormalities during pre-tests in warm conditions, it quickly became apparent that the contact to the superconductors deteriorated during the test campaign in liquid nitrogen. We suspect that in the area of the soldered contacts, flux ran between the HTS tapes by capillary action, leading to an oxidation of the tape surface. The forces occurring during the measurements may have caused a displacement of voltage taps just sticking loosely in the tape stacks. This manifested itself in an increasing, high noise. The voltage signal of pole 2 of SC section 1 was so noisy that an evaluation was not possible throughout the whole test campaign. Strongly scattering data points obviously caused by noise were masked for a clearer view. The voltage signal of pole 1 in SC section 3 shows a slight resistive increase up to 3270 A, but its values are far below the E-field criterion of $1 \mu\text{V}/\text{cm}$. Above this current, a sharp voltage increase was initially seen, after which the values fell back to the original, slightly rising curve. Since the voltage signal was very noisy, it is not possible to say with final certainty whether the increase was merely caused by bad contacts or whether there was a current redistribution that caused the signal to increase for a short time. Above 3390 A, a stronger noise occurred, which can possibly be explained by the fact that the current was changed in smaller steps and also reduced and increased several times in between. The voltage drops at the 180° - and 90° -joints of pole 1 and 2 are shown in Figure 9 versus the applied current. The voltage drops measured at the maximum currents of 3450 A correspond to resistances of $1.86 \text{ n}\Omega$ and $1.84 \text{ n}\Omega$ for the 180° joints of pole 1 and 2, respectively and to resistances of $2.93 \text{ n}\Omega$ and $3.62 \text{ n}\Omega$ for the 90° -joints of pole 1 and pole 2, respectively. These values are well below the maximum design values of $5.6 \text{ n}\Omega$ which correspond to ohmic losses of 1 W at $I=13.33 \text{ kA}$.

4.2. Length change

For DC test #3, the current was first increased in 50 A steps from zero to 1000 A and then kept constant. At constant current, the superconductor section 2 between the 180° - and the 90° joints of the demonstrator cable was stretched by 7 mm, i.e. by $\Delta L/L=0.38\%$. A negative influence of the stretching of the cable on the voltages different sections of the cable could not be observed. Even after stretching, the cable demonstrator easily carried the nominal current of 3.3 kA.

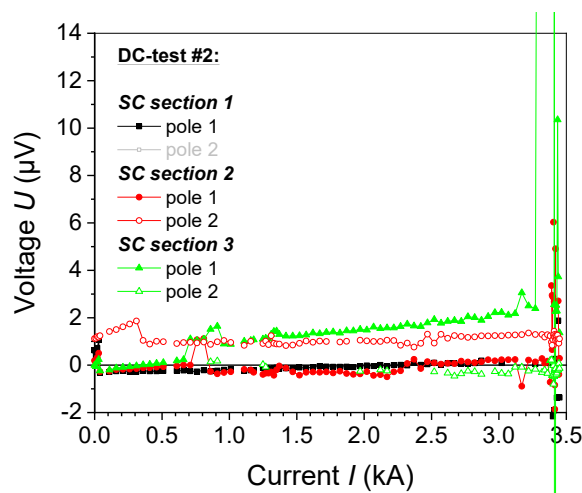


Figure 8: Voltages measured at the SC sections of the 2-pole cable versus applied current.

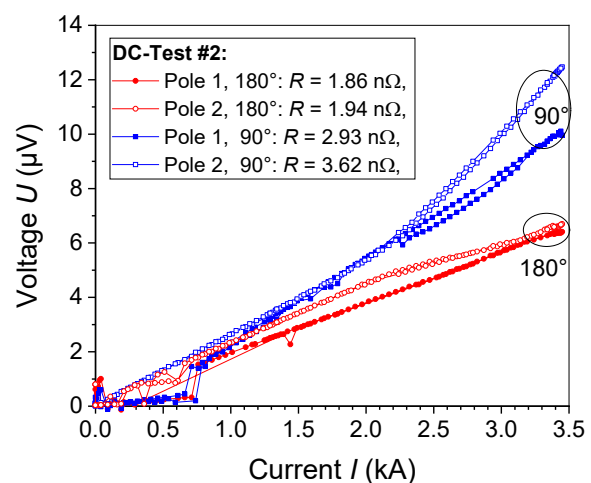


Figure 9: Joint voltages measured during DC test #2 versus current.

4.3. Lorentz force test

Following DC test #3, a Lorentz force test was carried out. The purpose of this test was to show that the cable is able to compensate the Lorentz forces occurring at a current of 13.33 kA. Since a current of 13.33 kA far exceeds the current-carrying capacity of the cable demonstrator at 77 K, AC currents of short duration (2 periods, 50 Hz) were applied in order not to heat up the conductor too much. The current amplitude was successively increased in several tests up to a maximum amplitude of 20 kA. Current and total cable voltage signals are shown in Figure 10 versus time. The maximum current amplitude of 20 kA corresponds to a maximum force per unit length of about 7.3 kN/m acting on the individual tape stacks (Figure 11). The low total voltages during the measurements with maximum currents of 0.843 kA and 1.392 kA were not measurable with the experimental setup due to the low resistivity of the cable system. Up to currents of 3.74 kA we observed a clear phase shift between current and voltage signal, indicating a non-negligible inductance of the entire circuit. In these ranges of maximum currents, the resistive part of the voltage signal is essentially caused by the resistive joints, since the resistivity of the REBCO tapes in the superconducting state is low (AC losses or incipient resistivity). In the measurements with a maximum current amplitude of 11.98 kA and higher, the phase shift becomes considerably smaller. However, the voltage curves do not show a sinusoidal behavior, but show a small shoulder. This behavior is probably due to the fact that the REBCO tapes are initially in the superconducting state at low currents, i.e. the resistivity of the system is low. As the current increases, the resistivity of the REBCO tapes increases strongly due to the critical current being exceeded, so that the voltage curve is essentially determined by the resistive component. In the measurements with the two highest maximum current amplitudes ripples appeared in the voltage signals. It is suspected that these ripples were caused by movement of the tapes near the short-circuit connection, where the tape stacks were laid over a short distance without formers.

The AC Lorentz-force test corresponds to a worst-case scenario since it is to be expected that the pulsating forces varying between zero and the maximum force represent a considerably higher load for the structure than slowly rising and falling forces occurring in the DC case.

4.4. Final DC tests

Following the Lorentz force test, further DC tests were carried out in order to rule out any damage to the superconductors. During DC test #4, a current ramp of up to 3500 A was applied to the cable. The voltages in the superconductor sections kept below the I_c -criterion although a slight increase was detected at currents above 3 kA. The voltage across the 90°-joint of pole 2 showed a steep increase at $I > 3.1$ kA, indicating a possible damage. Nevertheless, the cable was still able to carry a higher current than the design current of 3.3 kA at 77 K. In a 5th DC test, a rapid voltage increase occurred in SC section 3 at a current of 3480 A, i.e. between the 90°-joint and the short connection of pole 1 and 2, resulting in

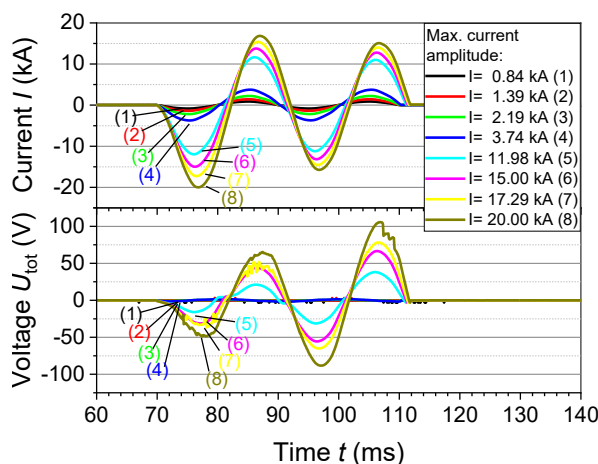


Figure 10: AC currents (50 Hz, 40 ms) and voltages versus time during Lorentz-force test.

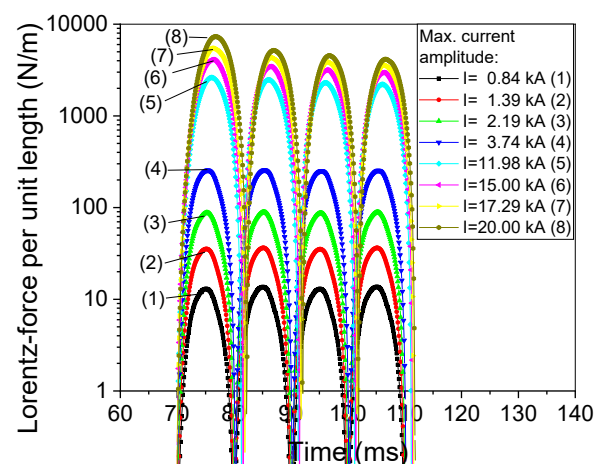


Figure 11: Calculated Lorentz forces on stacks versus time during Lorentz-force tests.

the destruction of the superconductor stack in this area. Possible causes for the occurrence of the defect include damage to individual tapes during the Lorentz force test. Damage was to be expected in SC section 3 in particular, as the SC stacks in this area were not supported by a support structure as in SC sections 1 and 2. In the area of SC section 3, only G10 supports were used to stabilize the contacts (see inset of Figure 7). The superconductor stacks themselves were free to move between the G10 supports and were strongly bent at the short connection. The screwed short-circuit connection between poles 1 and 2 proved to be another weak point. The resistance was more than $12 \mu\Omega$, resulting in a heating power of 120 W at $I = 3.5$ kA. Heating effects may have led to the destruction of SC section 3 of pole 1. The long sections 1 and 2, supported by the regular 3D printed structure, definitely were not affected.

5. Summary

We developed and tested a 2-pole DC busbar for power transmission in hybrid-electric propulsion systems for aircraft. Two application cases were considered for a voltage level of 3 kV: transmission of 10 MW electrical power with nitrogen cooling ($T \approx 70$ K) and transmission of 40 MW with hydrogen cooling at $T = 20$ -25 K. We developed a 3D-printed support structure that allows compensation of thermal length changes and withstands the high Lorentz forces occurring at currents of 13.33 kA and higher. A demonstrator cable with 180° and 90° joints was tested at 77 K in LN_2 . The critical current was above 3.3 kA and the resistive losses of single joints were below 1 W. A length change $\Delta L/L = 0.38\%$ at $I = 1$ kA did not deteriorate the cable properties. An AC Lorentz force test with AC currents up to 20 kA was successful in the regularly supported parts of the cable.

6. References

- [1] Lee D S 2018 Available: https://assets.publishing.service.gov.uk/government/uploads/system/uploads/attachment_data/file/813342/non-CO2-effects-report.pdf
- [2] Ansell P J and Haran K S 2020 *IEEE Electrification Magazine* **8** 18-26, June 2020
- [3] European Commission 2011, Flightpath 2050 Europe's Vision for Aviation. Report of the High Level Group on Aviation Research, doi: 10.2777/50266
- [4] Boll M, Corduan M, Biser S, Filipenko M, Pham Q H, Schlachter S, Rostek P and Noe M 2020 *Supercond. Sci. Technol.* **33** 044014
- [5] Jones C E, Norman P J, Galloway S J, Armstrong M J and Bollman A M 2016 *IEEE Trans. Appl. Supercond.* **26** 3601409
- [6] Zermeno V M R, Quaiyum S and Grilli F 2016 *IEEE Trans. Appl. Supercond.* **26** 4901607 HTS modeling workgroup. [Online]. Available: <http://www.htsmodelling.com/?p=917>
- [7] Zermeno V M R, Habelok K, Stepień M and Grilli F 2017 *Supercond. Sci. Technol.* **30** 034001 http://www.htsmodelling.com/?page_id=748 - Jc_B_theta
- [8] Wimbush S C and Strickland M N 2017 *IEEE Trans. Appl. Supercond.* **27** 8000105 Wimbush S and Strickland N 2016 A high-temperature superconducting (HTS) wire critical current database. figshare. Collection. <https://doi.org/10.6084/m9.figshare.c.2861821.v12>
- [9] Stafford B H, Sieger M, Ottolinger R, Meledin A, Strickland N M, Wimbush S C, Van Tendeloo G, Hühne R and Schultz L 2017 *Supercond. Sci. Technol.* **30** 055002 (7pp)
- [10] Gouge M J, Demko J A, Roden M L, Maguire J F and Weber C S 2008 *AIP Conf. Proc.* **985**, 1343-50
- [11] Park Y, Lee M, Ann H, Choi Y H and Lee H 2014 *NPG Asia Mater.* **6** e98
- [12] Bagrets N, Augieri A, Celentano G, Tomassetti G, Weiss K-P and della Corte A 2015 *IEEE Trans. Appl. Superc.* **25** 6602705.

Acknowledgment

The authors acknowledge funding of the TELOS project by the German Ministry of Economic Affairs and Energy under Grant-No. 20Y1516C. We dedicate this paper to our colleague Andrea Kling who passed away recently. We thank her for supporting us in mounting the cable demonstrator.